Dissociative excitation of H_2, HD, and D_2 by electron impact

B. L. Carnahan and E. C. Zipf
Department of Physics and Astronomy, University of Pittsburgh, Pittsburgh, Pennsylvania 15260
(Received 22 January 1976; revised manuscript received 28 March 1977)

Time-of-flight techniques have been used to investigate the electron-impact dissociation of H_2, HD, and D_2 in order to determine the effect of isotopic mass variation in the target molecule on the dissociative excitation process. At incident electron energies near 100 eV, the time-of-flight spectrum produced from each molecule was found to consist of atoms in the metastable $2s$ state and in high-lying, long-lived Rydberg levels. The individual time-of-flight distributions, kinetic-energy spectra, and relative differential cross sections for these two species resulting from each molecule have been measured. In several instances these results were found to vary significantly between the three isotopic forms. In particular, the kinetic-energy spectrum of the Rydberg atoms produced from dissociative excitation of H_2 was notably dissimilar in shape from the corresponding distributions produced from HD and D_2. Also the $2s$ and Rydberg production cross sections differed between the three molecules, being less in both cases for HD and D_2 than for H_2. In the dissociation of the heteronuclear HD molecule, it was found that the ratio of fast H($2s$) atoms to D($2s$) atoms was about 1 to 1, while the same ratio comparing the Rydberg atoms was nearly 2 to 1. These differences indicate the influence of the mass variation on the position of the Franck-Condon region in the production of $2s$ atoms and on the competition between autoionization and dissociation in the formation of Rydberg fragments.

INTRODUCTION

Dissociative processes play an important role in the ionization balance and thermal economy of a planetary atmosphere because they are a copious source of metastable atoms and ions, kinetically energetic particles, and extreme-ultraviolet photons. In previous experiments performed in this laboratory optical, quenching, and time-of-flight techniques have been used to determine the identity and to measure the kinetic-energy distributions of the products created by electron-impact dissociation of O_2, N_2, CO_2, NO, NO_2, N_2O, and CH_4.[1-10] These studies show that molecular dissociation involves a multitude of competing processes in which doubly excited states and predissociation via forbidden channels often play decisive roles. In order to investigate these processes further, we have undertaken a comparative study of the production of metastable and long-lived Rydberg atoms by electron-impact dissociation of H_2, HD, and D_2, a family of gases where possible isotopic effects are likely to be most pronounced.

The results of this study can be summarized as follows. For production of $2s$ atoms a similar kinetic-energy spectra was observed for each isotopic form of the hydrogen molecule, but the relative production cross sections decreased as the isotopic mass increased. For Rydberg atoms it was found (i) that the kinetic-energy spectrum from H_2 was significantly different than that from D_2 and HD, (ii) that contrary to the predictions of the core ion model, the Rydberg and ion energy distributions resulting from the dissociation of H_2 agreed only moderately well although a greater degree of similarity was found when the same comparison was made for the D_2 results, (iii) that the Rydberg production cross sections also decrease with increasing molecular mass, and (iv) that for the dissociation of HD, where the ratio of fast H($2s$) atoms to fast D($2s$) atoms was 1 to 1, the same ratio comparing fast H(Ryd) atoms to D(Ryd) atoms was 2 to 1. The observed variation in the $2s$ production cross section is apparently the result of shifts in the position of the Franck-Condon region among the three isotopic derivatives due to the differing nuclear masses. Dissimilarities in the shapes of the Rydberg spectra indicate that the principal production channels through which these species are formed in HD and D_2 are less important for H_2 where other channels seem to dominate. This may reflect the influence of the mass differences on competing autoionization and dissociation processes.

APPARATUS

A detailed description of the time-of-flight apparatus used in this investigation has appeared in several previous publications.[8,9] Only a brief review of the system will be presented here with particular attention given to the alterations made in the apparatus for this study. The experiment is shown schematically in Fig. 1. A magnetically focused electron gun produces a pulsed beam of electrons (typically 0.4 μsec in duration) that is directed through a collision chamber which serves as a diffuse gas source. Metastable fragments formed by electron excitation of the target gas diffuse through a slit in the side of the collision

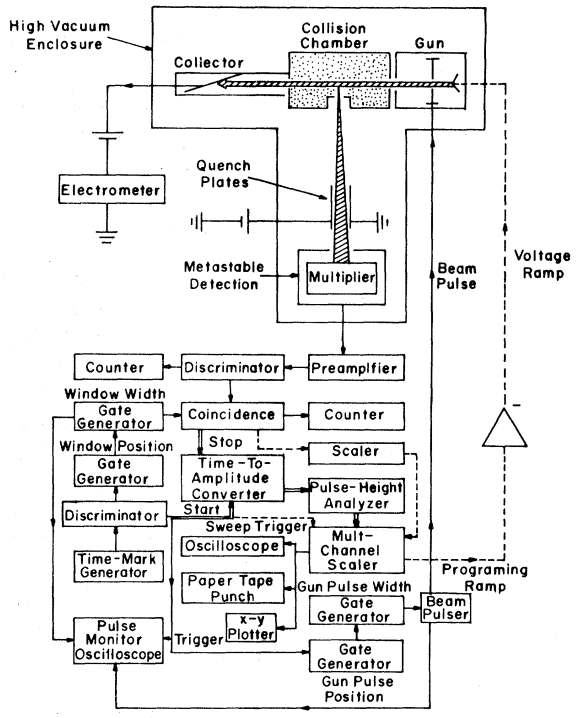

FIG. 1. Apparatus schematic. Solid lines, coupling between electronic components common in all data runs; double lines, time-of-flight runs.

chamber and ultimately are incident on a Cu-Be surface detector positioned at 90° to the electron beam path. Data were collected at several collision cell to detector spacings, although the principal time-of-flight (TOF) distance employed was 28.0 cm.

In order to separate the 2*s* and Rydberg signals an electrostatic field capable of quenching all 2*s* metastables was introduced in the transit region. This field was developed between a set of plates positioned parallel to and equally spaced on either side of the line of sight from the center of the collision cell exit slit to the center of the detector (see Fig. 1). At the 28.0-cm TOF distance these plates extended from 3.7 to 11.0 cm in front of the detector and were separated by a distance of 2.5 cm.

The detector used in this study was sensitive to charged species as well as metastable and Rydberg fragments. As the detection of non-neutrals was undesirable, it was necessary to exclude these species from reaching the detector. Due to the action of the magnetic field used to collimate the electron beam, charged species were prevented from making a straight-line transit from the interaction region to the detector. In order to check the effectiveness of this barrier, an electrically insulated wire mesh was inserted directly behind the quenching plates, parallel to the detector face. By floating this mesh to various potentials both above and below ground, it was possible to determine if any charged fragments were in fact reaching the detector. The results from a number of such tests demonstrated that the magnetic field was sufficient to eliminate charged fragments from the particle beam entering the detector.

EXPERIMENTAL PROCEDURES

The measurements attempted in this work were based on first separating the atomic 2*s* and Rydberg signals and then determining the time-of-flight spectra of these two species for each of the three molecules along with the relative production cross sections. The following discussion is a brief review of the experimental techniques used to acquire this data.

A. Separation of the 2*s* and high Rydberg signals

Over the range of incident electron energies used in this study (between 50 and 150 eV) the excited neutral products resulting from dissociative excitation of H_2, D_2, or HD will contain atoms in the metastable 2*s* state and highly excited long-lived Rydberg levels, both of which possess sufficient internal energy to initiate a pulse in the detector. In order to separate these overlapping signals, an electrostatic field was introduced in the transit region between the detector and collision cell. A range of electrostatic field strengths exists which will readily quench a 2*s* metastable to the ground state while producing a negligible effect on a Rydberg atom. The separation of the 2*s* and Rydberg signals was accomplished through the accumulation and subtraction of data recorded with and without an appropriate field present in the transit region. In an electrostatic field of strength F V/cm, the 2*s* and 2*p* levels of the hydrogen (or deuterium) atom are mixed, reducing the 2*s* lifetime from its field free value of $\frac{1}{7}$ sec to a value given by[11]

$$\tau_{2s}(F) = 1/2780F^2 \text{ sec}.$$

Thus even for a beam of very fast 2*s* atoms (kinetic energy ≃10 eV), transit through a region only a few centimeters in length where a field on the order of 50 V/cm was present would quench all but a few percent of the originally excited atoms.

A similar electrostatic field applied to a beam of Rydberg atoms will not greatly alter their radiative lifetimes as these are determined by the numerous intermediate transitions required for such atoms to deexcite and not from the metastability of a particular level. While the mixing caused by the field will change slightly the transition prob-

abilities between states, calculations of the effective radiative lifetimes for the hydrogen atom as the result of multiple transitions from highly excited levels have shown these values to be equally long in both the field free and Stark field cases.[12,13] At the same time, while field ionization in an electrostatic field could also depopulate a beam of Rydberg atoms, the probability of this occurring for the bulk of the atoms is slight at low field strengths. It has been shown that field ionization will not occur until a critical field strength is reached, the required field strength value being proportional to the inverse fourth power of the principal quantum number of the particular Rydberg atom.[14] For the present work we estimate that at the highest quenching fields used (~60 V/cm) only Rydberg atoms with $n>50$ will be ionized. As the relative Rydberg production cross section is proportional to n^{-3} and as Donohue *et al.*[15] have shown that after a 20-cm flight path the population of Rydberg levels from dissociation of H_2 peaks at an n value between 15 and 18, the percentage of the Rydberg signal which would be lost due to field ionization should be negligible.

The effect of an electrostatic field on the time-of-flight distributions produced from H_2, HD, and D_2 can be seen in Fig. 2. Part (a) of this figure shows the field free distributions while part (b) contains the spectra recorded under identical conditions but with a field of 60 V/cm present across the quenching plates. Apart from the photon and background signals, the data presented in Fig. 2(a) represent the composite 2*s* and Rydberg distributions, while the spectra presented in Fig. 2(b) are due to the Rydberg atoms. The 2*s* spectra were obtained by subtracting two such sets of data.

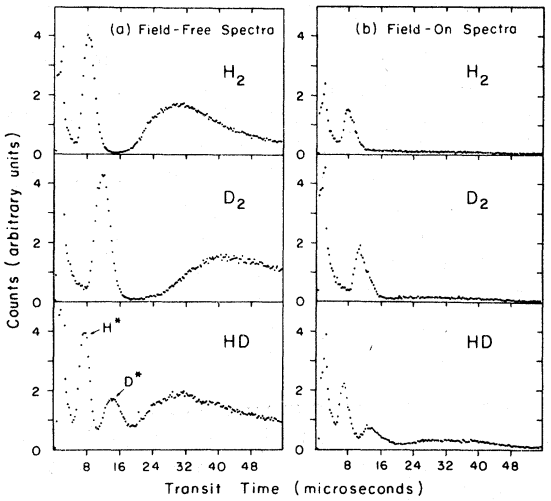

FIG. 2. Time-of-flight distributions of the atomic metastable fragments resulting from the bombardment of H_2, D_2, and HD by 100-eV electrons as observed at 90° to the primary beam and 28.0 cm from the collision region: (a) the total metastable spectra recorded with no fields introduced by the quenching plates; (b) the Rydberg spectra recorded with the 2*s* metastables attenuated due to a field of 60 V/cm present across the quenching plates.

B. Relative measurements

In order to determine the relative 2*s* and Rydberg production cross sections, it was necessary to normalize the observed signal intensities for both species with respect to those experimental conditions which varied between runs, namely, the incident electron beam current and source density in the collision cell. The electron beam current active in the interaction region was taken to be that measured by the Faraday cup and this value, monitored continuously, varied by less than 5% over the course of a given run. It was assumed that dividing the Faraday cup reading into the observed counting rate would properly normalize the signal level with respect to the electron beam current.

The density in the collision cell was not directly measured but was rather inferred from the pressure measured in the delivery line between the gas handling manifold and the collision cell. Although this value was not monitored continuously due to possible dissociation of the gas by the ion gauge, readings were taken before and after each run and again were consistently within 5% of each other. It was found that a given delivery line pressure would correspond to a particular main chamber pressure for all three gases over the range of delivery line pressures used. The main chamber pressure P for free molecular flow is given by[16]

$$P=F/S\,,$$

where F is the flow of gas out of the collision cell and S is the pumping speed. The flow between the collision cell and main chamber is given by $\frac{1}{4}N\bar{V}A$,[16] where N is the number density in the collision cell, $\bar{V}$ is the average molecular speed, and A is the escape area of the slit in the collision cell. Although $\bar{V}$ will vary as the inverse square root of the mass, the pumping speed has a similar mass dependence[16] and thus for equal pressures to exist in the main chamber for two gases of different mass, the densities in the collision chamber must be equal. Combined with the previously mentioned relationship between the main chamber and delivery line pressures, this implies that the particle density of HD or D_2 molecules in the collision chamber would be the same as that for H_2 if the respective pressure readings in the delivery line were equal.

To obtain data that could be directly compared between the three gases, a particular delivery

line pressure was chosen and the respective counting rates for each gas were recorded at the value. As the density in each case was the same, the relative counting rates, after current normalization, represented the relative production cross sections. A set of such relative values were obtained at a number of delivery line pressures and averaged to yield the final values.

In comparing the observed counting rates between excited atoms with differing velocities, it was assumed that the detector efficiency depended only on the internal excitation of the atom and not its velocity. All 2*s* atoms and all Rydberg atoms were assumed to have constant, although different detection efficiencies. While this has not been directly verified for the species detected in this study, it has been shown in several instances that ejection of electrons from metal surfaces due to the impact of neutral atoms will not occur until a threshold kinetic energy for the impacting fragment is reached which is typically in excess of 100 eV.[17-20] As even the fastest atoms in the present study have translational energies well below this level, the influence of variable fragment velocity on detection efficiency would seem to be negligible.

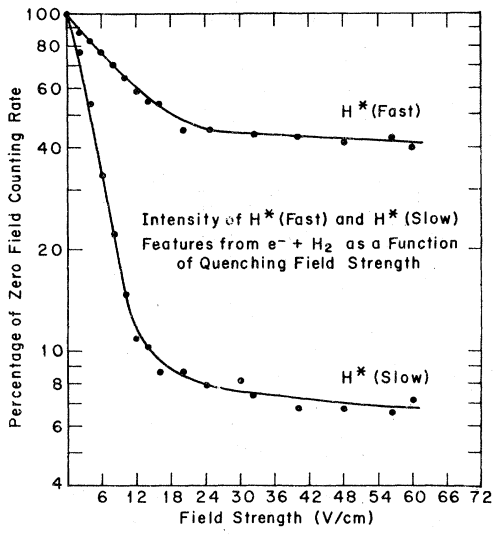

FIG. 3. Attenuation due to the presence of an electrostatic field in the transit region of the fast and slow metastable hydrogen atoms resulting from the excitation of H_2 at an incident energy of 100 eV.

RESULTS

A. 2*s* and Rydberg kinetic-energy distributions

The time-of-flight distributions presented in Fig. 2(a) exhibit the two-component velocity distributions for excited atoms resulting from dissociation of H_2 and D_2 which has previously been observed by several authors.[21-25] For HD the conservation laws require that the H atom velocity be twice that of the D atoms, a fact readily apparent in the fast-atom distribution but hidden due to the overlap between the H and D atom signals in the slower-atom spectrum. When potentials were applied to the quench plates it was found that in each case the signal due to the slower atoms was attenuated to the background level whereas the fast-atom spectrum retained a residual unquenched component. The fractional quenching as a function of field strength is shown in Fig. 3 for H_2, which characterizes the behavior for all three gases. The time-of-flight spectra recorded with a field strength of 60 V/cm present across the plates are shown in Fig. 2(b). As described earlier the observed effect of the electrostatic field was interpreted as a selective quenching of the 2*s* atoms, which means that the distributions presented in Fig. 2(b) are due to only long-lived highly excited Rydberg atoms. The residual distribution arriving in the vicinity of the slow feature in the field on HD spectrum is thought to be due to the detection of metastable nitrogen atoms present in the HD gas sample as an impurity.

By using the quenching techniques the 2*s* and Rydberg time-of-flight distributions from each gas were obtained. The respective kinetic-energy spectra for these fragments are related to these time-of-flight distributions through Eq. (1),

$$P_e(t)\,dt = P'_e(\epsilon)\,d\epsilon\,, \tag{1}$$

where t represents the fragment arrival time, ϵ the fragment kinetic energy, subscript e the incident electron energy, $P_e(t)$ is the normalized probability distribution for a fragment's arrival between times t and $t+dt$, and $P'_e(\epsilon)$ is the normalized probability distribution for detection of a fragment with a kinetic energy between values $\epsilon + d\epsilon$. Due to the relationship between the arrival time and the kinetic energy, Eq. (2),

$$\epsilon = \tfrac{1}{2}MD^2/t^2\,, \tag{2}$$

where M is the fragments' mass and D the time-of-flight path length, the energy differential can be written as $d\epsilon = -(MD^2/t^3)\,dt$ so that Eq. (1) becomes

$$P_e(t)\,dt = P'_e(\epsilon)(k/t^3)\,dt$$

or

$$P'_e(\epsilon) = P_e(t)t^3/k\,, \tag{3}$$

where k is a constant. Using this result, the kinetic-energy distributions were obtained from the time-of-flight data by multiplying the TOF results

by a t^3 factor and then replotting these distributions with the time scale appropriately converted to a kinetic-energy scale.

The major limitations on this technique arise first from the background signal level and secondly from imprecision in the time or length measurements. Due to the t^3 factor, even a small background signal can produce large erroneous features in the energy spectra. This problem is most serious for the low-velocity tail of a distribution where the difference between the background and desired signals is blurred and the appropriate background subtraction becomes difficult to assess. Errors in the time and length measurements are carried over into the energy scale through Eq. (2). The time measurement introduces the largest uncertainty as time zero, taken as the center of the prompt photon pulse which is essentially coincident with the gun pulse, will be uncertain by the half width of this pulse. Because the exact position of $t=0$ becomes increasingly important in establishing the fragment kinetic energy as that energy increases, the uncertainty in the energy scale introduced by even a narrow gun pulse width will be large. Operationally, the time-of-flight path length used primarily in this work (28.0 cm) was chosen in part to mitigate this effect while maintaining adequate signal levels.

In Figs. 4–6 the TOF distributions of the fast metastable fragments produced from H_2, D_2, and HD have been replotted as kinetic-energy spectra. For HD, due to scatter in the time-of-flight data, a 5-point first-order least-square routine was applied to smooth the distributions somewhat. The sharp features evident in the HD distributions are artifacts from this process and are not reproducible features of the actual distribution.

The distributions in Fig. 4 are the energy spectra of the fast atomic fragments produced from H_2 and D_2 at 100 eV. The top distribution in each case is that which was observed in the field free configuration. The bottom distribution is that due to the fast Rydberg atoms with the 2s signal quenched out. The middle distributions were obtained by subtracting the Rydberg signal from the field free distribution, and thus corresponds to the distribution of fast 2s atoms. As indicated by these plots the 2s distributions from H_2 and D_2 appear almost identical. However, there are noticeable differences between the two Rydberg distributions. The hydrogen distribution appears as one broad feature centered near 6.5 eV, with some hint of structure at 4.2, 5, and 8 eV. The deuterium distribution has two readily identifiable features centered near 5 and 7 eV and appears somewhat narrower than the hydrogen spectrum, particularly in the low-energy shoulder.

Figure 5 is a composite of the fast 2s atom distributions recorded for HD at incident energies of 75, 100, and 150 eV. As indicated in this figure the H(2s) atoms have twice the translational energy of the D(2s) fragments due to the mass differences. There is no indication of structure in these distri-

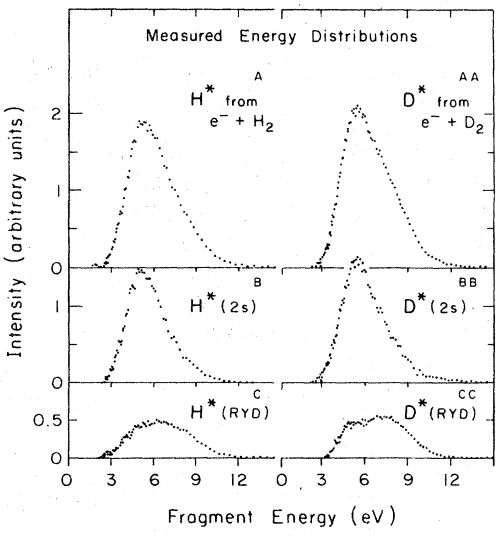

FIG. 4. Kinetic-energy spectra for the fast atomic metastable species resulting from the excitation of H_2 and D_2 at an incident energy of 100 eV.

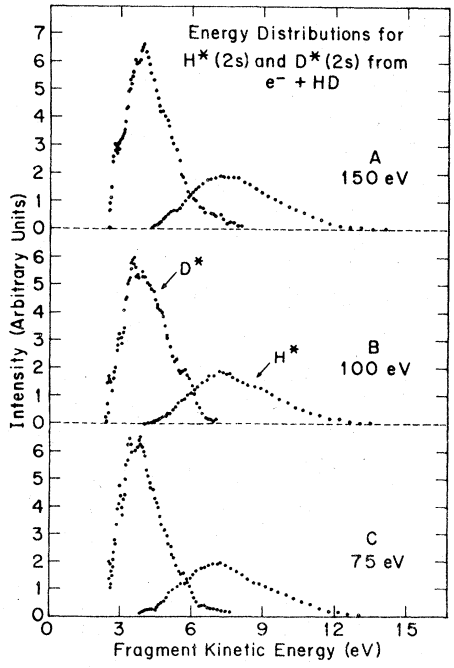

FIG. 5. Kinetic-energy spectra of the fast hydrogen and fast deuterium 2s atoms resulting from the excitation of HD at several impact energies.

butions beyond the central peak at each energy. In Fig. 6 the energy distributions of fast H(Ryd) and D(Ryd) atoms observed at 75, 100, and 150 eV are compared. Again the mass difference between the two atoms results in the hydrogen fragments having twice the energy of the deuterium fragments. The H(Ryd) distribution at 75 eV has two discernible features, centered at 6 and 9.5 eV. There is a perceptible shift in the positions of these features towards higher energies as the incident electron energy is increased. There also appears to be two structures in the D(Ryd) distributions at 75 eV, a shoulder area located between 2.5 and 3.5 eV, along with the central peak located between 4 and 5 eV. The position of these features also shifts noticeably to higher energies in the distributions recorded at 100 and 150 eV.

B. Relative production rates

The values used in comparing the production cross sections for the 2*s* and Rydberg atoms were obtained in two stages. First, for each molecule, a ratio was established between the signal intensity of the fast Rydberg atoms and that of the fast 2*s* atoms. These ratios were obtained from the time-of-flight data after the appropriate background signals had been subtracted. Then, using the techniques of coincidence counting, the total 2*s* signal from each gas was measured at a number of particular delivery line pressures for reasons discussed earlier, and then normalized with respect to the Faraday cup current. Total 2*s* signal levels recorded at equal source densities were compared and averaged yielding the relative 2*s* production rates, which when combined with the previously measured 2*s* to Rydberg ratios, yielded the relative Rydberg production rates. These values represent in effect the relative differential production cross sections for dissociative excitation of these three molecular isotopes by 100-eV electrons at an observation angle of 90° to the primary beam.

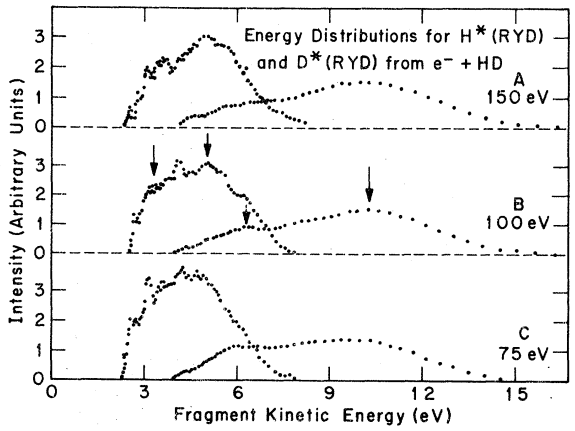

FIG. 6. Kinetic-energy spectra of the fast hydrogen and fast deuterium Rydberg atoms resulting from the excitation of HD at several impact energies.

In Table I the relative 2*s* production rates are presented. For each molecule the ratio of the fast 2*s* signal to total 2*s* intensity was determined from the observed difference between the field-off and field-on counting rates using coincidence counting techniques. As can be seen in the first column, this ratio was nearly 12% for each molecule. The last column, comparing the total 2*s* production rates, reveals that there is some variation in this value between the three molecules. The ratio quoted for HD contains the contribution from both the hydrogen and deuterium metastable fragments. In the first comment of this table the production ratio of fast H(2*s*) to fast D(2*s*) atoms for HD is computed and found to be nearly equal. The absolute differential cross section for both fast and slow 2*s* production from H_2 at 100 eV is given in the second comment of Table I.

In Table II the relative production rates for the fast Rydberg atoms are presented. The first column gives the ratio of the fast Rydberg signal to the fast 2*s* signal for each molecule as derived from the time-of-flight data. Again H and D components have been added together in the case of HD. Using this ratio and the data in Table I the relative production rates of the fast Rydberg fragments are computed in the center column of Table II. The third column is a list of the relative velocities of the fast fragments assuming that the energy shared between the dissociating atoms of each molecule is the same. The ratio of the fast H(Ryd) signal intensity of the D(Ryd) signal intensity at 100 eV from HD was nearly 2 to 1 as shown in the first comment of Table II. The individual H(Ryd) and D(Ryd) relative production ratios are computed in the second comment, each scaled by a factor of 2 to compensate for the dis-

TABLE I. Summary of relative differential cross sections for production of 2*s* metastables. All results were recorded at an incident beam energy of 100 eV. The ratio of the fast H(2*s*) to fast D(2*s*) from e^-+HD at 100 eV is 1.21±0.12. The total absolute differential cross section for the production of H(2*s*) due to electron impact on H_2 is $d\sigma(100\text{ eV})/d\Omega = 4.5\times10^{-19}$ cm^2/sr.

System	Fraction of total 2*s* signal due to fast 2*s* atoms at 100 eV	Relative cross section for the total 2*s* atom production at 100 eV
e^-+H_2	0.13±0.02	1.00
e^-+HD	0.12±0.02	0.87±0.13
e^-+D_2	0.12±0.02	0.87±0.09

TABLE II. Summary of production rates and relative velocities for fast Rydberg fragments. All results were recorded at an incident beam energy of 100 eV. The ratio of fast H(Ryd) to fast D(Ryd) from e^- + HD at 100 eV is 1.98 ± 0.22. The absolute differential cross section for $H_2 + e^- \rightarrow H(Ryd)_F$ at 100 eV is $d\sigma(100\text{ eV})/d\Omega = 8.8 \times 10^{-21}$ cm^2/sr.

System	Fraction of the fast fragments which are Rydberg atoms at 100 eV	Relative cross sections for production of fast Rydberg atoms at 100 eV	Velocity of the fast fragments relative to the fast H atom from H_2
e^- + H_2	0.15 ± 0.02	1.00	1.00
e^- + HD	0.17 ± 0.04	0.92 ± 0.19 [a]	1.155 (H) 0.577 (D)
e^- + D_2	0.15 ± 0.02	0.76 ± 0.12	0.707

[a] The individual H(Ryd) and D(Ryd) cross sections, scaled by a factor of 2 are

$\sigma(H) \times 2 = 0.92 \times 0.664 \times 2 = 1.22 \pm 0.24$,

$\sigma(D) \times 2 = 0.92 \times 0.336 \times 2 = 0.61 \pm 0.12$.

tinguishability of fragments in the HD case. The absolute total differential cross section for production of fast Rydberg atoms from H_2 at 100 eV is given in the final comment of Table II.

The uncertainties associated with the values quoted in Tables I and II are an indication of the amount by which the various individual measurements deviated from the final average values, and the potential inaccuracy of the relative density measurements in the interaction region for those measurements comparing the production rates for a particular species between two target gases. The uncertainty of the absolute 2*s* cross section value is limited primarily by the accuracy of the absolute density measurement and by our estimate of the sensitivity of the *MM*-1 mesh multiplier used as a detector,[26] while the Rydberg cross section is somewhat more uncertain due to lifetime effects. The absolute values quoted are probably reliable to within a factor of 2.

It is important to keep in mind that the values presented in Table I and II represent only the relative and absolute quantities as observed at 90° in the laboratory frame of reference. It is known that the angular distribution of H(2*s*) atoms and H^+ ions resulting from the electron bombardment of H_2 as observed in the lab frame are anisotropic.[24,27,28] A different angular distribution of dissociated fragments might be expected for each isotopic form of the hydrogen molecule as the variation in mass should result in a differing electron momentum transfer to each molecule at a given electron energy. As the angular dependence of the various signal levels was not investigated in the present study, no attempt has been made to adjust Tables I and II for any possible distortions due to differing degrees of anisotropy in the fragment distributions.

DISCUSSION

The production of 2*s* atoms from H_2 has been investigated by several authors and the principal channels involved have apparently been identified.[21-25] For electron energies in excess of 50 eV the chief production mechanisms contributing to the slow 2*s* metastable signal are excitation to several vibrational levels of the $D^1\Pi_u$ state and subsequent predissociation through the $B'^1\Sigma_u^+$ level, and direct excitation to the dissociative levels of the $B'^1\Sigma_u^+$ state. The fast atoms produced over the same range of electron energies are the result of dissociative excitation to the doubly excited $^1\Pi_u$ state. This level was identified and its shape in the Franck-Condon region derived in the results of several investigations similar to the present study.

In Fig. 7, the kinetic-energy distribution of the fast 2*s* atoms produced from H_2 as measured by

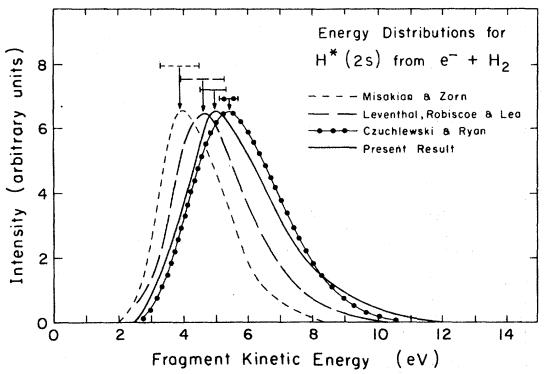

FIG. 7. Three previous measurements (Refs. 23, 24, and 25) of the kinetic-energy spectrum for the fast H(2*s*) atoms resulting from the excitation of H_2 compared with results from the present study. The relevant experimental conditions are discussed in the text.

Leventhal *et al.*,[23] Misakian and Zorn,[24] Czuchlewski and Ryan,[25] and in the present study are compared. Several of the experimental conditions are not identical in each case as the incident electron energies were 60, 70, 80, and 75 eV for the data of Leventhal *et al.*, Misakian and Zorn, Czuchlewski and Ryan, and the present study, respectively, while the observation angle was 80° in the data of Misakian and Zorn but 90° in the other three cases. At these electron energies the variation in the shape of the 2*s* distribution should be small but may shift Leventhal's results to somewhat higher energies. The difference in observation angle may also influence these results; however, there is some disagreement on this point. Measurements by Leventhal *et al.* indicate that more low-energy fragments are observed at 77° than at 90°, which may have the effect of shifting Misakian and Zorn's result to higher energies. While none of these spectra agree exactly, the general character of the fast 2*s* atom distribution as indicated by each result is largely the same. The principal source of the nominal discrepancy between these measurements is believed to be due to the uncertainty in the time scale and the effective time-of-flight path lengths. The bars shown on these curves indicate the extent of the uncertainty in the respective energy scales.

As noted earlier, measurements of the relative 2*s* intensities revealed that the total production rates for D_2 and HD were nearly 13% less than that observed for H_2. The only other determination of the relative 2*s* production cross sections which has been reported is that by Vroom and De Heer.[29] In their measurements of the atomic emission spectrum resulting from excitation of H_2 and D_2, they observed that the quenched 2*s* Lyman α signal from D_2 was 20% less intense than for H_2 as were the 2*p* Lyman α and Balmer α, β, γ, and δ lines which they also observed. Recently Khayrallah[30] measured the following emission ratios for several Balmer lines resulting from the excitation of H_2 and D_2 at 100 eV: for Balmer $\alpha \sim 1.06$, for Balmer $\beta \sim 1.11$, and for Balmer $\gamma \sim 1.19$. There are no similar measurements with which to compare our HD results.[31]

In their analysis, Vroom and De Heer attributed the bulk of the 2*s* signal to the fast fragments. As the excited states leading to these fast atoms lie in the ionization continuum of the molecule, the decrease in 2*s* production from D_2 to H_2 was thought to be due to a velocity-dependent competition between dissociation and autoionization of these levels. As the deuterium molecule requires a slightly longer time to dissociate than does the H_2 molecule, the probability of autoionization in D_2 is enhanced relative to H_2. Thus fast D^+ ions would be more likely formed than H^+ ions, or from the other point of view, the H(2*s*) atoms would be more likely formed than would the D(2*s*) atoms.

Our results show, however, that for each of these molecules, the fast peak contributes only 12% of the total 2*s* signal. The variation in 2*s* cross section must then be associated chiefly with the slow fragments rather than the fast, and thus competition between dissociation and autoionization should not play a large part in determining the total production rate of 2*s* atoms from these molecules. Alternatively the observed variation in the total 2*s* cross section may be a consequence of the small differences in the magnitude of the vibrational constants for ground state H_2, HD, and D_2 molecules. This variation in turn alters the range over which the Franck-Condon region intercepts the upper levels leading to the 2*s* atoms. Hence for HD and D_2, the distribution of vibrational levels of the excited molecular states, which are populated in the excitation process may give rise to more bound excited molecules and less predissociation and direct dissociation than for H_2.

With regard to the production of 2*s* atoms from HD, it was noted that the production rates for fast H(2*s*) and D(2*s*) atoms at 100 eV were nearly equal. The equality of the H(2*s*) and D(2*s*) signals suggests that the major process involved is excitation to a discrete excited level of the molecule followed by dissociation where either fragment is equally likely to be formed as the metastable species. The molecular level involved is most likely the $^1\Pi_u$ state identified by Misakian and Zorn[24] as being responsible for the fast 2*s* atoms near onset.

The production of highly excited Rydberg atoms through dissociative excitation of H_2 has only recently been investigated and as yet the principal production mechanisms involved have not been well defined. In the study by Schiavone *et al.*,[32] slow as well as fast atomic Rydberg fragments were observed to result from the excitation of H_2, and corresponding features presumably exist in the distributions produced from D_2 and HD. The failure to observe these slow Rydberg atoms in the present study is probably attributable to the broadness of the respective time-of-flight spectra and low absolute production rates which effectively buried these signals in the background. The detection method used by Schiavone *et al.* employed a detector positioned out of the metastable beam which was sensitive only to the Rydberg fragments. This method of operation has an inherently greater signal-to-noise ratio for Rydberg species than in our apparatus where the detector is sensitive to a much larger group of excited fragments and lies in the line of sight of the primary beam.

In terms of the core ion model, dissociative

excitation of molecular targets leading to the formation of Rydberg atoms proceeds through the excitation of a single electron of the ground-state molecule into a molecular Rydberg level which lies only slightly below the potential energy curve of the corresponding molecular ion.[33,34] Assuming the Rydberg curve has the appropriate shape, the molecule then dissociates as if it were in the ion level except that the Rydberg electron is captured into a high n orbit of what would otherwise be an ionized fragment. For H_2 (or HD and D_2) the only levels of this type are those which converge to the $^2\Sigma_g^+$ ground state of the molecular ion.[35] Due to the position of the Franck-Condon region, excitation to the dissociative region of these levels will result in the production of low-energy fragments and such processes are presumably the source of the slow Rydberg atoms.[32]

As dissociation through the singly excited levels can lead only to slow fragments, the production of more energetic Rydberg atoms must involve excitations to doubly excited levels. The core ion model would predict that a major production channel for the fast Rydberg atoms should proceed via dissociative excitation through molecular Rydberg levels converging to the first excited state of the H_2^+ ion, the repulsive $^2\Sigma_u^+$ level. Dissociative ionization through this level results in a distribution of protons centered near 8 eV,[27,28,36-38] as can be seen in the two representative measurements of the H^+ ion energy spectra resulting from the electron bombardment of H_2 which are presented at the top of Fig. 8. For comparison purposes, the lower panel of this figure contains two measurements of the H(Ryd) energy spectra resulting from H_2, recorded at electron beam energies and observational angles similar to those used in obtaining the ion distributions. While the details of the ion spectra differ, both exhibit structure in the range of higher kinetic energies which characterize dissociations through the $^2\Sigma_u^+$ level. On the other hand, the lack of a similarly positioned feature in the Rydberg spectra indicates that for H_2, contrary to the core ion model, the contribution of Rydberg levels converging to the $^2\Sigma_u^+$ state to the atomic Rydberg signal is minimal.[38]

In contrast to the H_2 results, there is evidence in both the D_2 and HD data that excitations to Rydberg states lying just below the $^2\Sigma_u^+$ level contribute strongly to the Rydberg spectra resulting from these two molecules. In Fig. 9, D^+ ion kinetic-energy distributions as measured by Stockdale[39] and the D(Ryd) spectra derived from data recorded in the present study are compared. Two ion distributions recorded at incident electron energies of 80 and 100 eV are shown while the Rydberg result is for excitation by 100-eV electrons. As il-

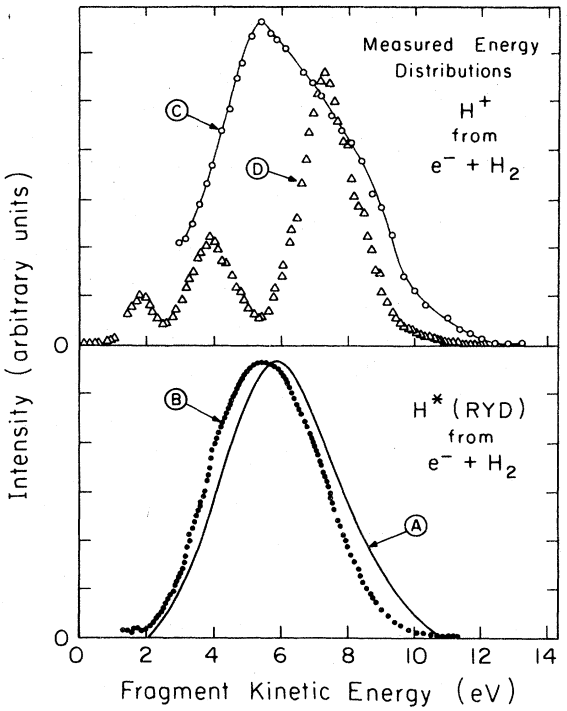

FIG. 8. Kinetic-energy spectra of the fast H(Ryd) atoms and H^+ ions resulting from electron bombardment of H_2. Rydberg spectra: curve A, distribution obtained in the present study as observed at 90° to a beam of 50-eV electrons; curve B, measurement by Schiavone *et al.* (Ref. 32) at the same observation angle and electron energy. Ion spectra: curve C, measurement by Van Brunt (Ref. 38), observed at 90° at a beam of 75-eV electrons; curve D, measurement by Crowe and McConkey (Ref. 37) observed at 27° to a beam of 50-eV electrons.

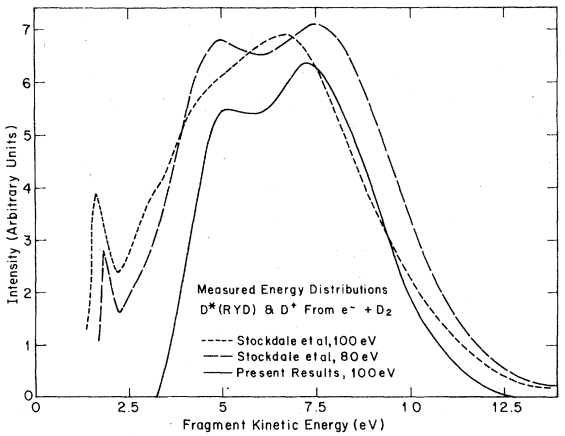

FIG. 9. Kinetic-energy spectra of the fast D(Ryd) atoms and D^+ ions resulting from the electron bombardment of D_2. Both the Rydberg distribution measured in the present study and the two ion spectra observed by Stockdale (Ref. 39) were recorded at right angles to the incident beam.

lustrated by these distributions, the alignment between features in the Rydberg and ion spectra is better than for H_2 and in particular the 8-eV ion peak is readily apparent in the Rydberg distribution.

While the energy distributions of the fast H^+ and D^+ ions produced from HD have not yet been measured, it is reasonable to expect that they are similar to the corresponding spectra resulting from H_2 and D_2 and will also exhibit a double peak structure. Using the conservation laws and assuming the same total dissociation energies for each molecule, the location of these features would be approximately 3 and 5 eV for the D^+ ions and 6 and 10 eV for the H^+ fragments, the more energetic ions in each case being the result of dissociation through the $^2\Sigma_u^+$ level. Comparison with the observed Rydberg spectra reveals that features at the positions of these predicted structures (indicated by the arrows in Fig. 6) are in fact present in the H(Ryd) and D(Ryd) distributions.

In addition to the structure resulting from excitations to highly excited level converging to the $^2\Sigma_u^+$ state, a second feature comprised of somewhat less energetic atoms is evident in the Rydberg spectra produced from both D_2 and HD although not in the H_2 results. While similar structures have also been observed in the ion distributions resulting from H_2 and D_2 (see Figs. 8 and 9), the data is as yet unclear as to which upper levels of the molecule are involved in the production of these ions. Crowe and McConkey[37] determined that these ions in the H_2 spectra were the result of excitations to doubly excited levels lying below the $^2\Sigma_u^+$ state which subsequently autoionize. Stockdale's[39] measurements for D_2 on the other hand revealed no evidence for the production of any fast ions below the energy necessary to excite the $^2\Sigma_u^+$ state, indicating that excited levels of the molecular ion are the source of these fragments. The corresponding features in the HD and D_2 Rydberg distributions are presumably the result of mechanisms paralleling those leading to these less energetic ions, although a more concise description of the production channel(s) involved cannot be made until further information regarding the onset energies for the Rydberg fragments is obtained. From the present results, however, it is possible to conclude that the process involved makes a substantial contribution to the Rydberg spectra from HD and D_2 but is a less important source of Rydberg fragments resulting from the excitation of H_2.

Summarizing then, the differences in shape between the energy spectra of the fast Rydberg atoms resulting from H_2 versus those produced from HD and D_2 appear to be the result of differing relative proportions with which the various production channels leading to Rydberg fragments contribute to the total distribution. Assuming that the same excited molecular levels are accessed with equal likelihood for each molecular isotope, then the relative success of certain of these channels in producing Rydberg atoms may depend strongly on the isotopic mass as this quantity affects the separation velocity. For instance, Schiavone *et al.*[32] have demonstrated that the onset energy for the production of the initial fast H(Ryd) atoms from H_2 is sufficient to excite only the low-lying, doubly excited members of the Rydberg series which converge to the H_2^+ $^2\Sigma_u^+$ level, i.e., states where the internal energy of the molecule is shared by both electrons more or less equally rather than by one electron promoted to a very high orbital as is the case for a higher-lying Rydberg level. Because both electrons in this group of states have low n values, their dissociation limits do not lead to the production of Rydberg fragments and hence the formation of a highly excited atom through such levels must depend on an additional process occuring as the molecule separates. Two such mechanisms have been suggested. As the dissociation through one of these doubly excited states progresses, a separation distance will eventually be reached where that state cuts across the $^2\Sigma_g^+$ ground state of the molecular ion. At this point there is some probability that the molecule may transfer to one of the Rydberg levels lying just below the $^2\Sigma_g^+$ level and complete the dissociation process as outlined by the core ion model. According to the Landau-Zener theory, the probability that a molecule dissociating along a repulsive diabatic curve will successfully cross a second molecular level and complete its dissociation along the first energy surface decreases as the velocity of the separating nuclei decreases.[40] Because the separation velocities for HD and D_2 are less than that of the H_2 molecule, it is more likely that the heavier molecular isotopes will fail to complete the multiple curve crossings required to reach infinite nuclear separation through the doubly excited level but will rather jump to either the $^2\Sigma_g^+$ level or Rydberg levels which converge to it, completing the dissociation along these curves. Hence production of Rydberg atoms following the excitation to one of the lower members of the series which converges to the $^2\Sigma_u^+$ state should be favored for HD and D_2 over H_2. While more detailed spectra are required at lower bombarding energies, the appearance of the Rydberg distributions at 100 eV would indicate that production through such levels is actually less prominent for HD and D_2 than in H_2, the opposite of what would be expected based on this first mechanism.

In an alternative model of Rydberg production through this group of states, one of the two low n value electrons autoionizes just prior to the crossing of the doubly excited level with the $^2\Sigma_g^+$ level and is then recaptured into a Rydberg orbital from which the molecule completes the dissociation again as described in the core ion model. Here the slower separation velocities of the HD and D_2 molecules may result in a higher ratio of autoionization to recapture than for H_2, as the success of the recapture process depends on a favorable matching between the relatively high velocity of the autoionizing electron and the slower velocity of the separating nuclei, a condition which is more likely to occur for H_2 than for the heavier HD and D_2 molecules.

In both of the above models, the production of Rydberg atoms competes with losses due to autoionization and the success of either in producing Rydberg atoms will depend on the ratio of the time required to reach the curve crossing point to the autoionization lifetime. The ratio of these time intervals will be smaller for HD and D_2 than for H_2 as the slower separation velocities of the heavier isotopes will extend the time they require to reach the curve crossing while the autoionization lifetime remains unchanged with molecular mass. Hence while the relative duration of these times may permit a finite number of such doubly excited molecules to dissociate to Rydberg fragments for H_2, a smaller ratio as for HD and D_2 may substantially decrease this probability.[41]

From the present results for HD and D_2 and from the measurements of Schiavone *et al.*[32] on H_2, it is clear that additional production channels through more highly excited molecular levels are involved in the production of Rydberg atoms as the bombarding electron energy is increased. While the preceding arguments deal only with the first group of states which contribute to the total Rydberg signal, the variation in separation velocity presumably continues to influence the competition between autoionization and dissociation for these higher molecular levels as well, which will in turn vary the relative production from these states between the members of the H_2-HD-D_2 system. Additionally the angular dependence on the shape of the Rydberg distributions may be important, particularly in the lower range of electron energies where the symmetry constraints outlined by Dunn[42] will introduce the greatest degree of anisotropy in the angular distributions of the dissociated fragments.

Finally as described earlier, the H(Ryd) and D(Ryd) spectra produced from HD seem similar in shape but differ by a factor of 2 in intensity. The enhanced production of the H(Ryd) atoms over the D(Ryd) fragments may be a consequence of the mechanism through which the molecular electron is captured by the dissociating nucleus to form a Rydberg atom. Depending on the type of process involved this electron is either in a relatively closely bound orbital around the molecule or in a large weakly bound molecular Rydberg orbit. In either case there is a period of time between the capture of the second electron around one of the two nuclei and the capture of the first electron in an atomic Rydberg orbit. During this time the Rydberg electron falls mainly under the influence of the temporarily charged nucleus. Thus in the case where the inner electron attaches to the D nucleus, the H nucleus moves rapidly away from the center of mass and consequently will influence the outer electron at an earlier time than in the reverse case where the inner electron attaches to the H nucleus, leaving the D nucleus momentarily charged. If the dissociation process is in competition with autoionization, the fact that the H nucleus can influence the outer electron at an earlier time than the D nucleus may be critical to the capture of that electron in a Rydberg state rather than for autoionization to occur.

ACKNOWLEDGMENTS

We would like to thank Dr. R. S. Freund for a number of helpful suggestions and Dr. R. J. Van Brunt for providing the results contained in Ref. 38 prior to publication. This research was supported in part by the National Aeronautics and Space Administration (NGL 39-011-030) and by the National Science Foundation (ATM75-21889).

[1]W. L. Borst and E. C. Zipf, Phys. Rev. A 4, 153 (1971).
[2]W. C. Wells, W. L. Borst, and E. C. Zipf, Chem. Phys. Lett. 12, 288 (1971).
[3]W. C. Wells and E. C. Zipf, Phys. Rev. A 9, 568 (1974).
[4]W. C. Wells, W. L. Borst, and E. C. Zipf, *Proceedings ICPEAC VII* (North-Holland, Amsterdam, 1971), p. 576.
[5]W. C. Wells, W. L. Borst, and E. C. Zipf, Trans. Am. Geophys. Union 52, 878 (1971).
[6]W. C. Wells, W. L. Borst, and E. C. Zipf, Bull. Am. Phys. Soc. 17, 397 (1972).
[7]W. C. Wells, W. L. Borst, and E. C. Zipf, J. Geophys. Res. 77, 69 (1972).
[8]W. C. Wells, W. L. Borst, and E. C. Zipf, Phys. Rev. A 14, 695 (1976).

[9]W. L. Borst and E. C. Zipf, Phys. Rev. A 3, 979 (1971).
[10]T. G. Finn, B. L. Carnahan, W. C. Wells, and E. C. Zipf, J. Chem. Phys. 63, 1596 (1975).
[11]H. Bethe and E. E. Salpeter, *Quantum Mechanics of One and Two Electron Atoms* (Springer-Verlag, Berlin, 1957).
[12]J. R. Hiskes, C. B. Tarter, and D. A. Moody, Phys. Rev. 133, A424 (1964).
[13]N. V. Fedorenko, V. A. Ankudinov, and R. N. Il'in, Zh. Tech. Fiz. 35, 585 (1965) [Sov. Phys.-Tech. Phys. 10, 461 (1965)].
[14]T. E. Ducas, M. G. Littman, R. R. Freeman, and D. Kleppner, Phys. Rev. Lett. 35, 366 (1975).
[15]D. E. Donohue, J. A. Schiavone, D. R. Herrick, and R. S. Freund, Bull. Am. Phys. Soc. 20, 1458 (1975).
[16]S. Dushman, *Scientific Foundations of Vacuum Technique* (Wiley, New York, 1962).
[17]M. Kaminsky, *Atomic and Ionic Impact Phenomena on Metal Surfaces* (Academic, New York, 1965).
[18]U. A. Arifov, R. R. Rakhimov, and Kh. Dzhurakulov, Dokl. Akad. Nauk SSSR 143, 309 (1962) [Sov. Phys.-Dokl. 7, 209 (1962)].
[19]D. B. Medved, P. Mahadevan, and J. K. Layfon, Phys. Rev. 129, 2086 (1963).
[20]P. M. Walters, Phys. Rev. 111, 1058 (1958).
[21]J. W. Czarnik and C. E. Fairchild, Phys. Rev. Lett. 26, 807 (1971).
[22]R. Clampitt, Phys. Lett. A 28, 581 (1969).
[23]M. Leventhal, R. T. Robiscoe, and K. R. Lea, Phys. Rev. 158, 49 (1967).
[24]M. Misakian and J. C. Zorn, Phys. Rev. Lett. 27, 174 (1971); M. Misakian and J. C. Zorn, Phys. Rev. A 6, 2180 (1972).
[25]S. J. Czuchlewski, Ph.D. thesis (Yale University, 1973); S. J. Czuchlewski and S. R. Ryan, Bull. Am. Phys. Soc. 18, 688 (1973).
[26]W. L. Borst, Rev. Sci. Instrum. 42, 1543 (1971).
[27]G. H. Dunn and L. J. Kieffer, Phys. Rev. 132, 2109 (1963).
[28]R. J. Van Brunt and L. J. Kieffer, Phys. Rev. A 2, 1293 (1970).
[29]D. A. Vroom and F. J. De Heer, J. Chem. Phys. 50, 580 (1969).
[30]G. A. Khayrallah, Phys. Rev. A 13, 1989 (1976).
[31]In the study by Czuchlewski (Ref. 25) the relative 2*s* production cross sections for dissociative excitation of the H_2-HD-D_2 system were measured for a bombarding electron energy of 80 eV. The yields for the slow 2*s* fragments from HD and D_2 were found to be 94% and 91%, respectively, of the slow 2*s* signal from H_2. At the same beam energy the number of fast H(2*s*) and D(2*s*) atoms resulting from the dissociation of HD were found to be equal.
[32]J. A. Schiavone, K. C. Smyth, and R. S. Freund, J. Chem. Phys. 63, 1043 (1975).
[33]S. E. Kupriyanov, Zh. Eksp. Teor. Fiz. 55, 460 (1969) [Sov. Phys.-JETP 28, 240 (1969)].
[34]R. S. Freund, J. Chem. Phys. 54, 3125 (1971); K. C. Smyth, J. C. Schiavone, and R. S. Freund, J. Chem. Phys. 59, 5225 (1973).
[35]T. E. Sharp, Potential Energy Diagram for Molecular Hydrogen and its Ions (Lockheed Palo Alto Research Laboratory LMSC-9, 1961).
[36]L. J. Kieffer and G. H. Dunn, Phys. Rev. 158, 61 (1967).
[37]A. Crowe and J. W. McConkey, Phys. Rev. Lett. 31, 192 (1973).
[38]R. J. Van Brunt, this issue, Phys. Rev. A 16, 1309 (1977). The contribution to the fast H(Ryd) spectrum from high Rydberg levels converging to the $^2\Sigma_u^+$ level may increase when the fragments are observed at angles other than 90°. Measurements by Van Brunt indicate that the intensity of the proton distribution produced from H_2 as the result of dissociation through the $^2\Sigma_u^+$ level is enhanced when the distribution is observed at angles parallel to the beam. As yet the possibility that a similar angular behavior accompanies the production of Rydberg atoms has not been investigated.
[39]J. A. D. Stockdale, V. E. Anderson, A. E. Carter, and L. Deleanu, J. Chem. Phys. 63, 3886 (1975).
[40]N. F. Mott and H. S. W. Massey, *The Theory of Atomic Collisions*, 3rd ed. (Oxford U.P., London, 1965).
[41]Using a classical model, Hazi has calculated that the fraction of D_2 molecules excited to the $^1\Sigma_g(2p\sigma u^2)$ level which reach the stabilization separation distance with respect to the $^2\Sigma_g(1s\sigma_g)$ state of the ion is slightly less than for H_2 (11% vs 14%). While the trend established by these calculations is in support of the present model, the variation would seem too small to totally account for the enhanced Rydberg production through this level for H_2 in comparison to HD and D_2. [See A. U. Hazi, J. Chem. Phys. 60, 4358 (1974)].
[42]G. H. Dunn, Phys. Rev. Lett. 8, 62 (1962).